CHEMICAL ENGINEERING TRANSACTIONS
VOL. 65, 2018

A publication of
AIDIC
The Italian Association of Chemical Engineering
Online at www.aidic.it/cet

Guest Editors: Eliseo Ranzi, Mario Costa

ISBN 978-88-95608- 62-4; **ISSN** 2283-9216

Biomass Combustion in a 140kW Fixed Bed Boiler: a Joint Experimental and Modeling Study

Federica Barontini[a], Chiara Galletti[a], Dario Di Mitri[a], Stefania Patronelli[a], Gianluca Caposciutti[b], Marco Antonelli[b], Umberto Desideri[b], Leonardo Tognotti[a]

[a]Dipartimento di Ingegneria Civile e Industriale, Università di Pisa, Largo Lucio Lazzarino 2, 56122 Pisa, Italy.
[b]Dipartimento di Ingegneria dell'Energia, dei Sistemi, del Territorio e delle Costruzioni, Università di Pisa, Largo Lucio Lazzarino 2, 56122 Pisa, Italy.
chiara.galletti@unipi.it

Computational Fluid Dynamics (CFD) modeling and experimental campaigns have been performed to investigate the performance of a 140 kW biomass fixed-bed boiler. The most widely used modeling approaches in literature, such as those representing the biomass bed as a single or a series of interconnected perfectly stirred reactors, were shown to be unsuited and affected by large uncertainties on the model definition. Indeed, point measurements just above the fuel bed, performed in this work, have shown that, despite the small bed dimension, temperatures are strongly not uniform. In the present work, a simple and efficient method to overcome these limitations is suggested by representing the biomass bed as a porous medium with sources and sinks of chemical species and energy. In this manner the impact of the primary air injection on the resulting field is taken into account. The predictions provide a satisfactory agreement with the available measurements, even though improvements have to be made especially for better describing the kinetics.

1. Introduction

In the last century the constant increase in energy consumption, especially fossil fuel energy, has led to a growth of greenhouse gas emissions and global warming issues. Biomass represents an attractive feedstock for energy production, being a widely distributed renewable and CO_2-neutral source. Small-scale boilers are the most widespread option, although further efforts on the design are needed to improve the boiler performance in terms of efficiency and emissions.
Computational Fluid Dynamics (CFD) may come to aid by allowing the consideration of different phenomena in complex geometries. However, high level-of-detail physical modeling requires high computational time and power, not always balanced by the numerous uncertainties that still affect the multi-phase combustion process (e.g., particle size and shape, moisture content, behaviour of the feeding system).
Therefore, two simplified CFD modeling strategies for biomass combustion in fixed-bed were proposed in literature. In both strategies only the gas-phase turbulent combustion in the combustion chamber (i.e., freeboard) is solved with CFD, while the biomass bed is cut off from the computational domain and its influence is taken into account by assigning boundary conditions to the CFD freeboard model. The first strategy directly employs experimental data to set up the aforementioned boundary conditions (Scharler et al., 2011), while in the second strategy a simplified bed model (e.g., a single or a series of perfectly stirred reactors) provides the inlet conditions for the CFD freeboard model (Yin et al., 2008; Galletti et al., 2016).
Both approaches would benefit of accurate experimental data above the biomass bed for a better model validation (Buchmayr et al, 2015) and, eventually, the set-up of boundary conditions. Moreover, as shown in a previous work (Patronelli et al., 2017), these models are strongly affected by the uncertainty on the inlet turbulence conditions that determine the turbulent mixing of volatile species and then reaction rates.
The purpose of this work is to obtain accurate measurements of temperature just above the fire pit of a small biomass fixed-bed boiler, with the aim to help the definition of a suitable CFD model. The idea is then to

develop a cheap model that has to be able to overcome the limitations of the above strategies. Such model can be further used to improve the design of the boiler and/or to optimize operating conditions.

2. Experimental setup

The experimental setup consists of an under-feed stoker boiler located at the Biomass to Energy Research Center (CRIBE) in Pisa. Biomass is fed into the combustion zone through a cochlea with a rotational speed of about 10 rpm. The total air flow is split into primary and secondary air; the primary air is fed through 68 rectangular holes placed laterally in the biomass bed while the secondary air is supplied through 9 injection pipes (see Figure 1a). Two hot wire flow-meters were used to measure the primary and secondary air flow rates. The combustion chamber was kept at a small depression of 20 Pa, through a fan placed at the flue gas outlet and controlled by a PID system. The flue gases pass through a gas to oil heat exchanger, providing thermal heat to the CRIBE utilities, and then through the flue-gas cleaning system.
The fixed-bed biomass boiler was provided with a measuring system that allowed collecting temperature and gas composition both above the fire pit and boiler outlet.
Different thermocouples were arranged along the whole plant to measure: the inlet air temperature, the flue gas and the oil temperatures both upstream and downstream of the heat exchanger. The thermocouple for the flue gas upstream of the heat exchanger was equipped with a shielded cap to minimize the radiative effects.
Many efforts were devoted for setting a measuring system able to capture the thermochemical field above the fire pit. In particular, six thermocouples were inserted and placed above the biomass bed in the positions indicated in Figure 1b. Moreover, a movable probe was used to sample the gas above the bed, where devolatilization products are predominant. A quantitative characterization of volatile products as CO_2, CO, H_2, CH_4, C_2H_6, C_2H_4 and C_2H_2 at different locations above the bed was carried out by the use of a micro-gas chromatograph and a Fourier Transform InfraRed Spectrometer (FTIR).
Finally, the flue gas composition was monitored by means of an Environnement S.A. station, equipped with infrared, paramagnetic, flame ionization, and chemiluminescence detectors. Further information about the experimental setup and instrumentation can be found in Caposciutti et al. (2017).
The experimental campaigns were performed by using different thermal inputs, air excesses, secondary to primary air flow ratios as well as types of biomass, in order to investigate the effect of operating conditions on the boiler performance.
In this work, however, only one experimental test is considered, performed with the coarse grain size (i.e. average particle diameter d_p = 13 mm) poplar wood chips, whose ultimate and proximate analyses are reported in Table 1. The total and primary air flow rates were 0.10 and 0.065 kg/s respectively (corresponding to a secondary to primary air flow rate ratio of 0.6), whereas the biomass flow rate was estimated to be approximately 0.033 kg/s.

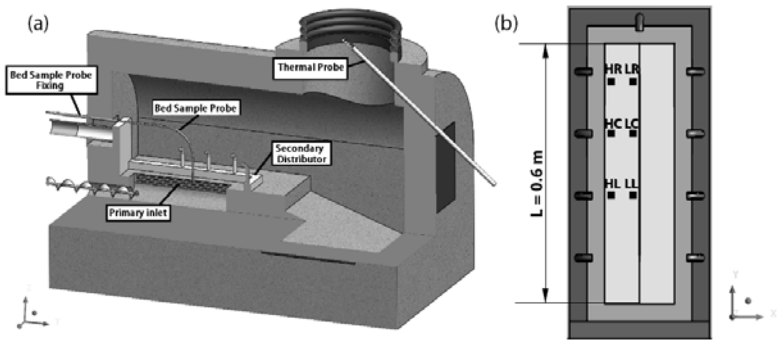

Figure 1: Scheme of the (a) biomass boiler and (b) thermocouples position on the bed (the biomass feeding is from the bottom).

Table 1: Ultimate and proximate analysis of poplar woodchips (daf = dry ash free, VM = volatile matter, FC= fixed carbon, LHV = lower heating value)

C	H	O	N	Moisture	VM	FC	Ash	LHV
[% daf]	[% daf]	[% daf]	[% daf]	[%]	[% dry]	[% dry]	[% dry]	[MJ/kg]
49.84	6.06	43.63	0.47	9.84	84.89	13.33	1.78	18.41

3. Numerical model

The numerical model is based on a single-phase turbulent reactive model in which the biomass bed is treated as a porous medium. This allows taking into account the injection of primary air (see Figure 2).
Hence the CFD model consists of two domains: one fluid domain for the freeboard (extending up to the bottom part of the heat exchanger, which is not included in the domain) and one porous domain for the fuel bed. The boiler symmetry allowed considering half geometry to reduce computational time. The discretization of the freeboard is made with a fully structured grid of about 800k elements, refined near the nozzles and obtained through O-grid strategy. Instead the biomass bed was discretized with a fully structured grid made of 10k cells.
The numerical simulations were carried out with ANSYS Fluent v.16 in which the Favre-Averaged Navier Stokes equations for a single-phase reactive turbulent flow were solved. The steady-state solution was obtained using a pressure-based solver that employs a second upwind interpolation scheme and a SIMPLE algorithm for pressure-velocity coupling.
The turbulence-chemistry interaction was considered through the Eddy Dissipation Model which assumes the chemical reaction rate to be infinitely fast, and hence turbulent mixing to control the reaction rates. Specifically, a two-step global reaction scheme was employed to describe volatiles oxidation to CO and CO_2; hence volatiles were treated as a pseudo-component, whose formula was derived from the biomass proximate and ultimate analysis:

$$
\begin{gathered}
C_{1.02}H_{2.04}O_{0.96}N_{0.00113} + 0.53\ O_2 \rightarrow 1.02\ CO + 1.02\ H_2O + 0.0056\ N_2 \\
CO + 0.5\ O_2 \rightarrow CO_2
\end{gathered}
\tag{1}
$$

The Reynolds stresses were estimated with the standard k-ε model and the radiative transfer with the P1 model, evaluating the gas spectral properties with the Weighted Sum of Gray Gas method.
Being a single-phase model, the drying, the volatiles release and char oxidation occurring inside the biomass bed were taken into account by employing volumetric source terms. Basically, these source terms are positive for volatiles, H_2O, CO_2 and energy, and negative (hence they are sinks) for O_2, that is consumed during char oxidation.
Such source terms are estimated through mass and energy balances on the biomass bed by assuming complete drying, devolatilization and char oxidation to CO_2. The amount of CO released from char oxidation could be neglected as indicated by the CO/CO_2 ratio estimated by the relationship of Tognotti et al. (1991).
As for the energy source, this was estimated by neglecting the contribution of volatiles oxidation. Moreover, a radiative source term was defined and was estimated through an iterative procedure that allowed updating the radiative heat transfer with the freeboard and boiler walls.
The source terms were not assigned uniformly across the entire fuel bed volume, as experimentally it was observed that the cochlea was unable to push the biomass up to the opposite edge of the fire pit with respect to the feeding. Hence, an attempt was made to take into account this maldistribution by setting full sources up to 85% of fire pit length and subsequently letting them to decrease linearly to zero in the last 15% of the fire pit length. Logically this procedure could be optimized.
The sources/sinks, were implemented through a C++ sub-routine by means of User Defined Function (UDF), coupled with the CFD code (Patronelli et al., 2018).
The porous model was defined by assigning a permeability of the bed, α, and an inertial coefficient, C_2, estimated by considering spherical particles, as:

$$\alpha=\frac{{d_p}^2}{150}\frac{\epsilon^3}{(1-\epsilon)^2} \tag{2}$$

$$C_2=\frac{3.5}{d_p}\frac{(1-\epsilon)}{\epsilon^3} \tag{3}$$

where ϵ is the void fraction and d_p is the average particle diameter. The above parameters were used to estimate pressure drops in the porous domain according to the Ergun equation:

$$\frac{|\Delta P|}{l}=\frac{1}{\alpha}u_\infty+\frac{1}{2}\rho C_2 {u_\infty}^2 \tag{4}$$

In the present investigation different values of the void fraction were considered, i.e. ϵ= 0.4, 0.5 and 0.6, in order to investigate the impact of these parameter on predictions.

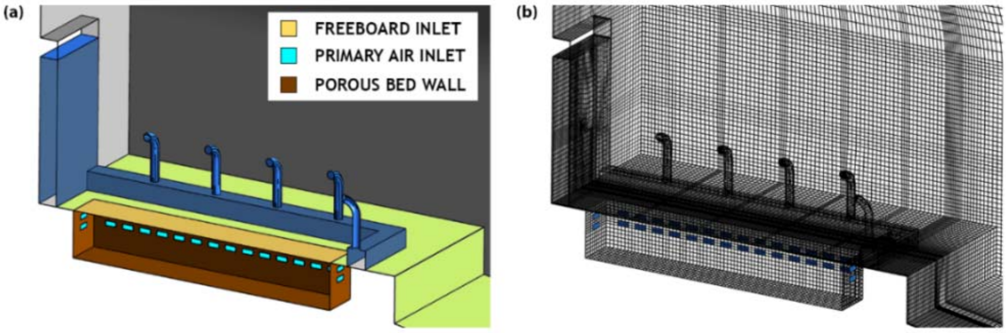

Figure 2: Details of the porous bed with primary air inlet (a) and grid (b).

4. Results

Figure 3 and Figure 4 show the temperature field in the longitudinal boiler mid-plane and different transversal cross-sections, respectively, estimated with different void fractions. The outlet experimental temperature is 687 K, whereas the predicted one (independently on the void fraction) is 693 K, thus in perfect agreement. As for chemical species, the measured and predicted O_2 mass fractions in the flue gas are 0.18 and 0.20, respectively. Such agreement on O_2 is considered very satisfactory, especially considering the many uncertainties that affect the boundary conditions (i.e., biomass mass flow rate, moisture content) to the model. The temperature distribution shows how the secondary air injection affects the morphology of the flame above the bed (see Figure 4). A previous work (Patronelli et al., 2017) indicated two adverse effects of secondary air on the thermal field: on one hand, increasing the secondary air leads to an increase of turbulent mixing and this favours reactions; on the other hand, the secondary air results in a quenching due to the presence of a cold flow. Indeed, the temperature field evidences the presence of a cold region above the fire pit, approximately at the center, while the high temperature region is pushed toward the fire pit edges, especially on the feeding side.

The comparison between the thermal fields in the boiler longitudinal mid-plane (Figure 3) obtained with different void fractions, apparently indicates higher temperatures in the biomass bed region with higher void fractions. However, the analysis of the 3D thermal field (Figure 4) highlights how, with increasing the void fraction, the primary air pushes more the reaction region toward the boiler symmetry plane. This can be observed from the temperature distribution on the horizontal plane just above the fire pit, used also for the experimental measurements (see Figure 5). The distribution is highly non-uniform for all void fractions, with temperature peaks near the symmetry plane and low temperatures near the side. For low void fraction, i.e. $\epsilon = 0.4$, a high temperature region is also noticed near the feeding, while for $\epsilon = 0.5$ and $\epsilon = 0.6$ the high temperature region is confined near the symmetry plane. This may be explained by considering that, in case of larger void fraction, the primary air, injected laterally, better penetrates the porous domain thus pushing reactants towards the symmetry plane and then generating an upward flow. Instead, the low void fraction leads to a more distributed flow in the porous domain with the presence of even a high temperature region near the feeding (Figure 5a).

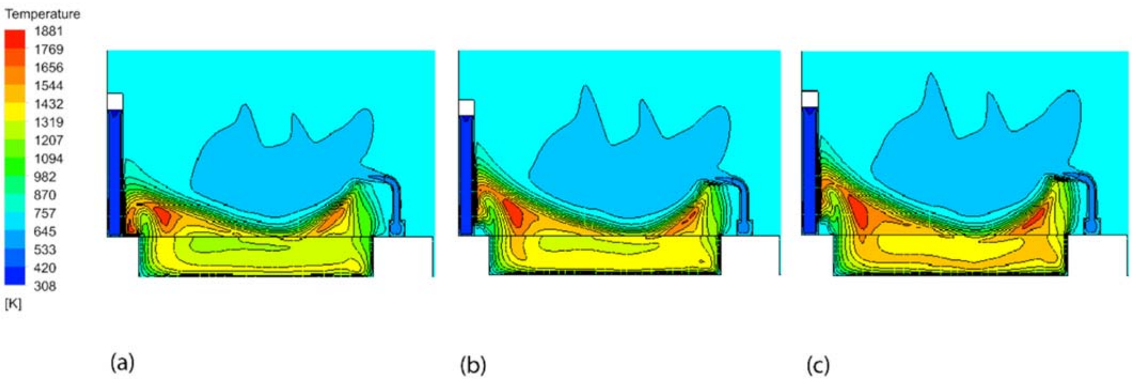

Figure 3: Temperature distribution in the boiler longitudinal mid-plane predicted with different void fractions of the porous domain: (a) $\epsilon = 0.4$; (b) $\epsilon = 0.5$; (c) $\epsilon = 0.6$.

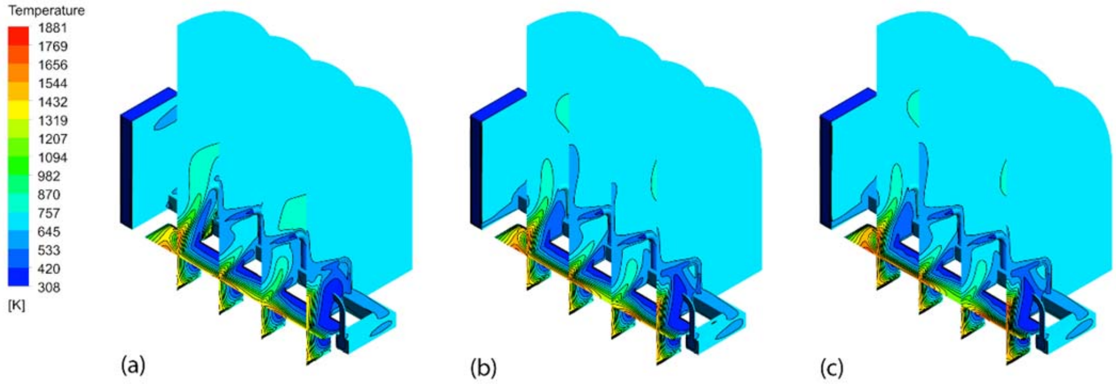

Figure 4: Temperature distribution in different boiler cross-sections and in the horizontal plane corresponding to the fluid-porous domain interface predicted with different void fractions of the porous domain: (a) $\epsilon = 0.4$; (b) $\epsilon = 0.5$; (c) $\epsilon = 0.6$.

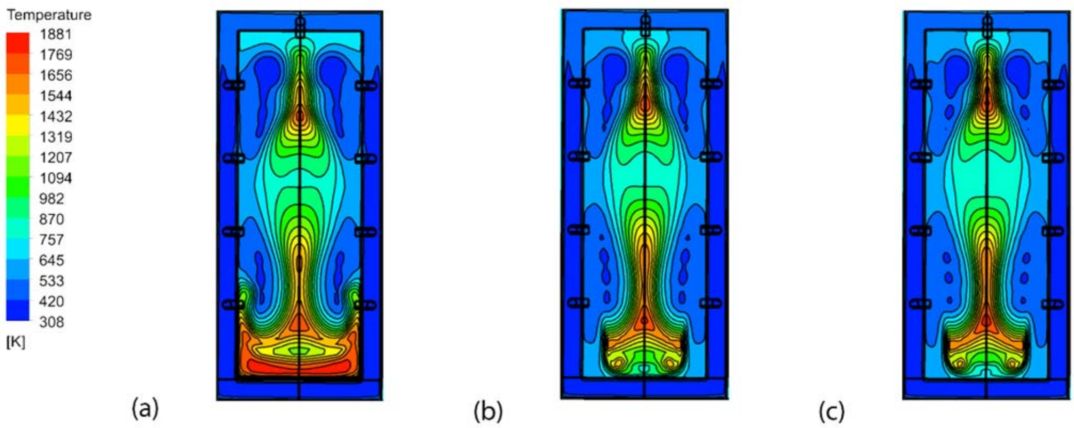

Figure 5: Temperature distribution in the horizontal plane above the fire pit (used also for experimental measurements) predicted with different void fractions of the porous domain: (a) $\epsilon = 0.4$; (b) $\epsilon = 0.5$; (c) $\epsilon = 0.6$.

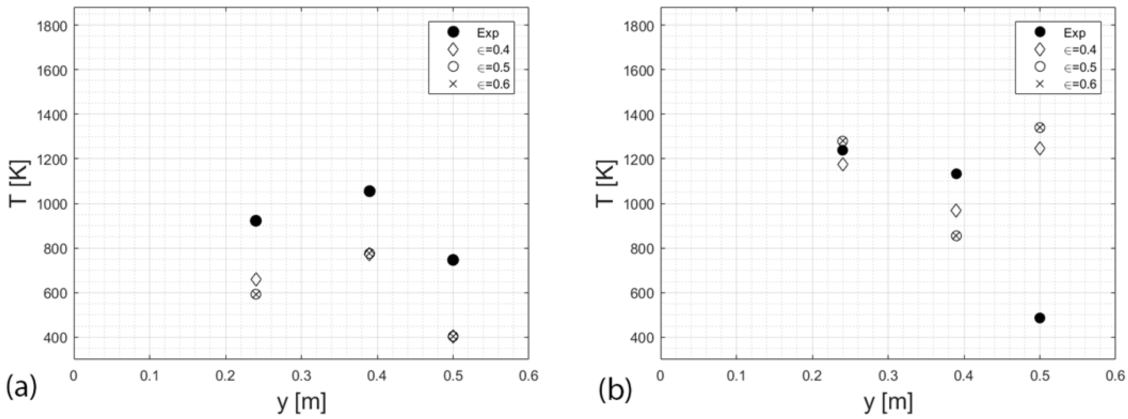

Figure 6: Comparison between experimental and predicted temperatures for different void fractions of the porous domain ϵ and locations: (a) HL, HC, HR (b) LL, LC, LR.

The experimental temperatures above the fire pit, shown in Figure 6 (see solid symbols), highlight also a large spatial variation, ranging from approximately 500 K to 1250 K. The comparison between predicted and measured temperatures is provided in the same Figure 6. At first glance, there is a systematic underestimation of the temperatures measured near the fire pit side (Figure 6a), although the trend is well captured. Some

improvement of the agreement between experiments and predictions can be observed in the HL position when reducing the void fraction, thus improving the primary air distribution in the porous region. As for the temperatures measured near the symmetric plane, a satisfactory agreement is obtained in the LL and LC locations, especially for the $\epsilon = 0.4$ case. Instead, the temperature measured in the LR position (far from the feeding) is very low, i.e., approximately 500 K, and such low temperature is not captured by the CFD model.
It is worth observing that high temperature gradients are present in all measurements locations (Figure 5) and these may affect the comparison between experiments and predictions. However, in the LR location, the very strong overestimation of temperature seems to indicate that the hypothesis of uniform sources/sinks across the domain (although reduced in the zone corresponding to the last 15% of fire pit length) has to be revised.

5. Conclusions

An experimental investigation on a small biomass fixed-bed boiler has indicated a significant spatial variation of temperature above the fire pit. Such variation cannot be considered with offline biomass bed models that are usually based on representing the biomass bed as a perfectly stirred reactor. In this work, the biomass bed is, instead, represented as a porous medium, with sources and sinks of chemical species and energy. This approach is computationally not expensive, as it is based on single-phase flow simulations. Approximately, a couple of days at maximum are needed for each test case when running on 8 cores (3.3 GHz Intel cluster). Furthermore, this approach allows to eliminate the uncertainty related to estimation of turbulence intensity and mixing, as well as to predict a not uniform temperature distribution, stemming from the primary air injection.
Preliminary tests were made to investigate the effects of the porous domain parameters, i.e. void fraction, on results. However future efforts will be needed to better characterise the porous domain, especially considering that biomass particles are not spherical and mono-sized. Moreover, the kinetics will be revised in order to validate and optimize the model using chemical species that were also measured above the fire pit.

Reference

Buchmayr M., Gruber J., Hargassner M., Hochenauer C., 2015, Experimental investigation of the primary combustion zone during staged combustion of wood-chips in a commercial small-scale boiler, Biomass and Bioenergy 81, 356-363.

Caposciutti G., Barontini F., Francesconi M., Antonelli M., 2017, Experimental investigation on the fixed bed of a small size biomass boiler, Energy Procedia 142, 468-473.

Galletti C., Giomo V., Giorgetti S., Leoni P., Tognotti L., 2016, Biomass furnace for externally fired gas turbine: development and validation of the numerical model, Applied Thermal Engineering 96, 372-384.

Patronelli S., Antonelli M., Tognotti L., Galletti C., 2018, Combustion of wood-chips in a small-scale fixed-bed boiler: Validation of the numerical model through in-flame measurements, Fuel 221, 128-137.

Patronelli S., Caposciutti G., Barontini F., Galletti C., Antonelli M., Desideri U., Tognotti L., 2017, Experimental and numerical investigation of a small-scale fixed-bed biomass boiler, Chemical Engineering Transactions, 57, 187-192.

Scharler R., Benesch C., Schulze K., Obernberger I., 2011, CFD simulations as efficient tool for the development and optimisation of small-scale biomass furnaces and stoves, 19th European Biomass Conference & Exhibition, June 2011, Berlin, Germany.

Tognotti L., Longwell J., Sarofim A., 1991, The products of the high temperature oxidation of a single char particle in an electrodynamic balance, Symposium (International) on Combustion 23, 1207-1213.

Yin C., Rosendahl L.A., Kær S.K., Clausen S., Hvid S.L, Hille T., 2008, Mathematical modelling and experimental study of biomass combustion in a thermal 108 MW grate-fired boiler, Energy Fuels 22, 1380-1390.